CHEMIJA. 2020. Vol. 31. No. 2. P. 77–86

Electrochemical investigations of the anticorrosive behaviour of the phosphated electrogalvanized steel additionally coated with conversion layer of cerium oxide

O. Girčienė*,

L. Gudavičiūtė,

A. Selskienė,

A. Kirdeikienė,

R. Ramanauskas

Center for Physical Sciences and Technology,
3 Saulėtekio Avenue,
10257, Vilnius, Lithuania

The anticorrosive behaviour of the electrogalvanized carbon steel with PZn, PZn-Ca and PZnNi phosphate layers additionally coated with the conversion layers of cerium oxide in chloride-contaminated media has been studied. The composition and structure of investigated samples were characterized by scanning electron microscope SEM, while the corrosion behaviour was investigated applying voltammetric and electrochemical impedance spectroscopy EIS measurements. The data obtained have shown that all investigated samples additionally coated with cerium oxide conversion coatings exhibited better protective abilities. To summarize the results of electrochemical and SEM measurements it was stated that the most porous (F = ~1–2%) PZnNi/Ce coating exhibited the best protective abilities in a chloride-contaminated solution. Therefore, cerium ions are able to penetrate into the substrate, which is zinc coated steel, through the open pores of the PZnNi layer.

Keywords: corrosion protection, phosphate coating, cerium oxide

INTRODUCTION

For a long time, steel surface modification by zinc coatings has been used to increase its corrosion resistance. The useful lifetime of zinc electrodeposits can be further increased by formation of a passive film on their surface. Chromate and phosphate films on metals are a common additional surface treatment used for various applications in different industrial fields. An excellent anticorrosive behaviour of chromate films is well known; however, the toxicity of Cr(VI) compounds restricts application of this technology [1, 2]. Phosphate coatings on metals are most commonly used for corrosion protection [3–6].

The phosphating of metals is a traditional surface treatment technique used for various applications in different industrial fields. As an important surface treatment method, phosphating has become so popular that it has been applied for aluminium, zinc and their alloys, cadmium, as well as for other metals. Phosphating is essentially an electrochemical phenomenon in which dissolution of the metal occurs at the micro-anode(s) and discharge of hydrogen followed by hydrolysis and precipitation of insoluble phosphates take

* Corresponding author. Email: olga.girciene@ftmc.lt

place at the micro-cathode(s). Zn phosphate coatings on Zn consist essentially of $Zn_3(PO_4)_2 \cdot 4H_2O$ (hopeite). Only in the case of formation of a Zn phosphate coating on Zn, the reaction is simple and the composition of the coating straightforward. The addition of cations, such as Ca, Mn and Ni, to $Zn_3(PO_4)_2 \cdot 4H_2O$ is an alternative to improve the resistance of the phosphate coatings in alkaline and acid environments [4–8]. Films from Ca modified Zn phosphate baths contain rhombic crystals of scholzite $Zn_2Ca(PO_4)_2 \cdot 2H_2O$, the proportion of the latter being directly related to the Ca content in the solution [4]. The presence of Ni^{2+} ions in the phosphating bath improves the corrosion resistance at the base of pores and accelerates the surface reactions during phosphating [10, 11]. The increase in phosphate layer mass with increase in Ni concentration was reported in the literature [10]. The elements such as Ni and Mn are used to increase the alkaline stability of phosphate layers [6, 7]. The authors [6, 7] have measured the rate of Zn, Mn and Ni phosphates leaching during exposure to an alkaline electrolyte. The results obtained demonstrate that the presence of Ni^{2+} in the phosphate bath increases the alkaline resistance of the top layer.

The main problem in application of phosphate coatings in aggressive media is the existence of open pores and pinholes [9, 12, 13]. The corrosion resistance of the phosphate coating is related to the size and population density of pores in the film. The pores provide a path for corrosion attack, leading to localized corrosion in an aggressive environment. As the corrosion reactions are initiated at the coating-substrate interface, determination of porosity is important to estimate the overall corrosion resistance of the coated materials [12].

Self-healing is defined as the ability of material or surface to automatically heal or repair damages. In a series of studies on the use of cerium ion in protective coatings, Hinton and Wilson [14] reported that the cerium ion, which acts as an inhibitor in solution, was as effective as the chromium ion. The action of the cerium ion resembled that of the chromium ion, and CeO_2 acted as a barrier film. When a defect was generated, a cerium ion in the film repaired it, due to dissolution from the film and oxidation of the defect site [15]. The study of cerium based conversion coatings on galvanized steel has shown the influence of anions, such as Cl^-, NO_3^-, SO_4^{2-} and CH_3COO^-, in a coating deposition solution on the corrosion behaviour of the formed film [16]. The results of electrochemical measurement and salt spray test indicate that the corrosion behaviour was greatly improved by the addition of SO_4^{2-} to the coating solution. It was supposed that the presence of SO_4^{2-} in the solution forms a complex between Ce^{3+} and SO_4^{2-}, which causes the incorporation of SO_4^{2-} into the cerium conversion coatings [17].

The aim of the present work was to investigate the anticorrosive behaviour of the phosphated electrogalvanized carbon steel additionally coated with the conversion layer of cerium oxide in chloride-contaminated media.

EXPERIMENTAL

Materials and sample preparation

Analytical grade chemicals were used for the preparation of electrodeposition and corrosion testing solutions. The working electrodes were steel samples with electrodeposited Zn coatings covered with phosphates and additionally with conversion cerium layers. An alkaline cyanide-free plating solution contained the following: ZnO – 10 g/l, NaOH – 100 g/l, accessories, 20–25°C. Zn coatings of 10 μm thickness were deposited at a current density (i) of 0.035 A cm^{-2}.

Three types of phosphating solutions were used for film formation under the conditions: PZn (Zn^{2+} – 0.17 M, PO_4^{3-} – 0.34 M, NO_3^- – 0.14 M, NO_2^- – 0.0025 M, pH = 2.2–2.5, t = 40–50°C, 10 min), PZnCa (Zn^{2+} – 0.12 M, PO_4^{3-} – 0.34 M, NO_3^- – 0.14 M, Ca^{2+} – 0.05 M, NO_2^- – 0.0025 M, pH = 2.2–2.5, t = 45–55°C, 10 min), PZnNi (Zn^{2+} – 0.17 M, PO_4^{3-} – 0.34 M, NO_3^- – 0.14 M, Ni^{2+} – 0.003 M, pH = 2.1–2.4, t = 50–55°C, 10 min). The phosphated samples were kept for 24 h under ambient conditions prior to the measurements.

The cerium conversion coating Ce was formed by a simple immersion of the samples for 10 min into the solution 0.05 M $Ce(NO_3)_3$ + 0.025 M Na_2SO_4, containing 3 vol.% H_2O_2 at room temperature.

Morphology and composition

The microstructure and elemental composition of specimens were studied by a scanning electron microscope (SEM). A Helios NanoLab 650 dual

beam workstation (FEI) with an X-Max 20 mm^2 energy dispersive detector (energy resolution of 127 eV for Mn Ka, Oxford Instruments) was used for imaging and energy dispersive analysis. The deposited film thickness analysis was performed on the produced and vacuum Pt coated cross-sections of the samples by the focused ion beam (FIB) technique.

Electrochemical measurements

The corrosion behaviour of samples was investigated in an aerated stagnant 0.5 M NaCl solution. The electrolyte was prepared from analytical grade chemicals and deionized water. All electrochemical measurements were performed at ambient temperature with an Autolab PGSTAT302 potentiostat using a standard three-electrode system with a Pt counter electrode and a saturated Ag/AgCl reference electrode. All potentials are reported versus the saturated Ag/AgCl reference electrode. The corrosion current densities (i_{corr}) were determined from voltammetric measurements by Tafel line extrapolation. A specimen was polarized with a potential scan rate of 0.5 mV s^{-1}, from the cathodic to the anodic region. The polarization resistance (R_p) values were determined from linear polarization measurements, which were performed between ±10 mV around E_{corr}, with a scan rate of 0.1 mV s^{-1}.

The measurements of electrochemical impedance spectra (EIS) were performed at the open circuit potential with the FRA2 module applying a signal of 10 mV amplitude in the frequency range of 20 kHz to 0.001 Hz. The data obtained were fitted and analysed using the EQUIVCRT program of Boukamp [18].

Electrochemical experiments were performed at least in triplicate.

RESULTS AND DISCUSSION

Surface morphology and composition

Phosphate conversion coatings

A variety of protective methods have been used to improve the corrosion resistance of carbon steel. The galvanized zinc coatings have a special place in industrial applications. Zn is more tolerant to enhanced chloride ion concentrations than steel, and where corrosion of metal does occur, Zn furnishes cathodic protection to steel. The useful life of Zn electrodeposits can be further increased by a passive film formation on their surface. Three phosphating solutions of different composition (PZn, PZnCa and PZnNi) were applied to grow protective coatings on the galvanized Zn surface. The surface morphology of zinc electrodeposits (Fig. 1) and the difference in the surface morphology of the phosphate coatings (Fig. 2) can be observed from the SEM images. The monocation PZn coating appeared to be compact, consisting of platelet shaped crystallites of 5–10 μm in length and 2–4 μm in width, which uniformly covered the surface of sample. The surface morphology studies, which were performed by SEM, revealed that the presence of Ca and Ni ions in the phosphating solution resulted in an increase in crystallite dimensions. The bication PZnCa coating structure is characterized by platelets with sizes up to 30 μm in length, while the PZnNi coating consists of the platelets, the dimensions of which varied between 10 and 40 μm (Fig. 2). The SEM image of the cross-section of PZnNi indicated the presence of the structural defects like open and closed pores in this layer (Fig. 3). The thickness of the phosphate layer is from 1 to 3.3 μm.

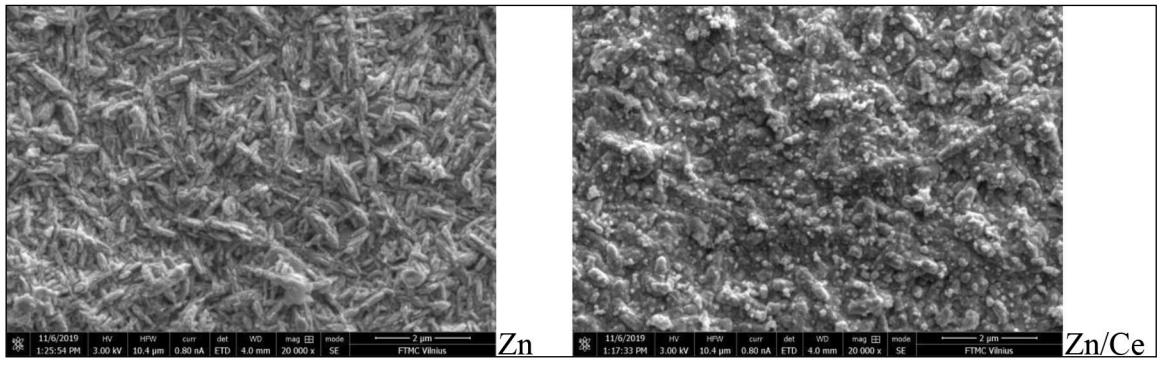

Fig. 1. SEM micrographs of the Zn and Zn/Ce samples

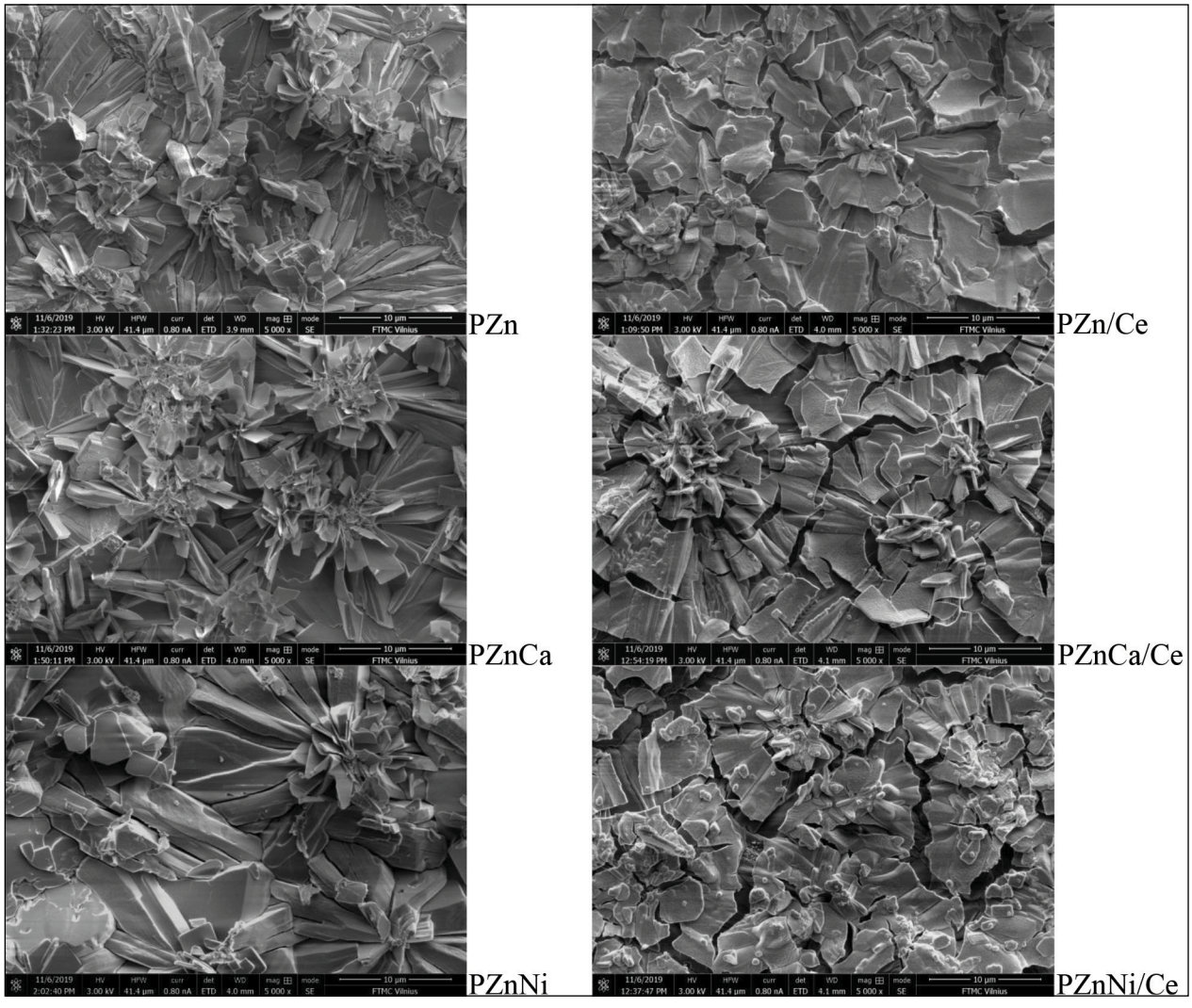

Fig. 2. SEM micrographs of the phosphated Zn samples without/with cerium coatings

The analysis of the elemental composition of phosphate layers was performed by EDS measurements. Its results listed in Table 1 indicated that the principal constituents of the phosphate coatings were as follows: the amount of O varied between 62.1 and 65.1 at.%, the amount of P varied between 9 and 9.6 at.% and the concentration of Zn varied between 25.2 and 28.6 at.%. The PZnCa and PZnNi coatings contained only ~0.2 at.% of Ca or Ni.

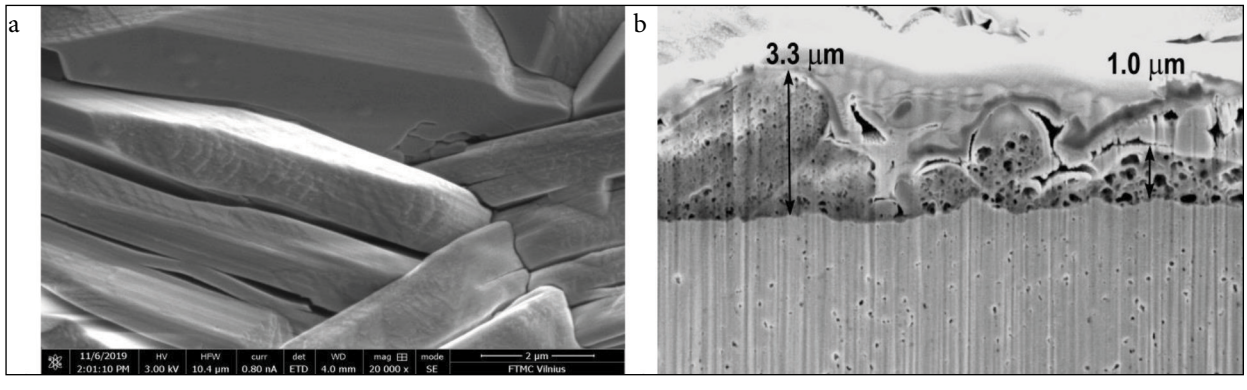

Fig. 3. SEM images of the microstructure (a) and the cross-section (b) of the PZnNi sample

Table 1. **The elemental composition of the investigated coatings systems**

Sample	Elements, at.% (by EDS)						
	Zn	O	P	S	Ce	Ca	Ni
Zn	85.56	14.44	–	–	–	–	–
PZn	27.38	63.6	9.02	–	–	–	–
PZnCa	28.58	62.11	9.14	–	–	0.17	–
PZnNi	25.16	65.07	9.58	0.01	–	–	0.18
Zn/Ce	59.85	39.3	–	0.05	0.8	–	–
PZn/Ce	22.68	65.49	8.83	0.96	2.04	–	–
PZnCa/Ce	21.48	65.72	8.82	1.27	2.65	0.15	–
PZnNi/Ce	24.39	64.1	8.41	0.95	1.99	–	0.16

Two layers cerium-phosphate conversion coatings

The phosphate coatings have superior corrosion resistances, but they present no evidence of having the ability to 'self-healing'. The self-healing properties, which allow durable protection even after a partial damage of the phosphate coating, can be achieved by introducing of cerium ions, which can impart an active corrosion protection ability to the phosphate coatings. The samples of Zn, PZn, PZnCa and PZnNi additionally coated with the conversion layer of cerium oxides were under investigations (Figs. 1, 2).

Cerium based materials are famous for their redox properties because of the conversion between Ce(III) and Ce(IV) valence states under oxidation-reduction conditions. The analysis of elemental composition of the investigated samples additionally coated with cerium layers was performed by EDS measurements, the results of which are listed in Table 1. The results of the analysis of Zn/Ce indicate that the amount of Ce was 0.8 at.%, whereas the amount of Ce of PZn/Ce, PZnCa/Ce and PZnNi/Ce samples reached 2–2.7 at.% (Table 1).

SEM images of the surface morphology of Zn/Ce and PZn/Ce, PZnCa/Ce and PZnNi/Ce are presented in Figs. 1 and 2. The layer of cerium on Zn is made of random located aggregates, which can be supposed to be precipitated Ce oxide compounds (Fig. 1). Whereas cerium oxide conversion coating on all phosphated samples exhibits a cracked 'dried river' morphology (Fig. 2).

Polarization measurements

The phosphate coating acts mainly as a mechanical barrier in corrosion processes [2]. During a polarization process the properties of substrate material do not change, so the anodic process of coated samples is the same as that of the non-coated one. The corrosion behaviour of the investigated samples was evaluated from the electrochemical measurements, which were carried out in a 0.5 M NaCl solution. The polarization curves of Zn, PZn, PZnCa and PZnNi electrodes without/with cerium oxide coatings are shown in Figs. 4 and 5. The electrochemical behaviour of the PZnNi layer on zinc-coated steel was less noble than the behaviour of the PZn ($Zn_3(PO_4)_2 \cdot 2H_2O$) layer (Fig. 4). The values of R_p of the investigated samples, which were determined from the linear polarization measurements ±10 mV around E_{corr}, are listed in Table 2. As seen from the data among all the investigated samples, PZnCa exhibited the smallest, whereas PZnNi the highest

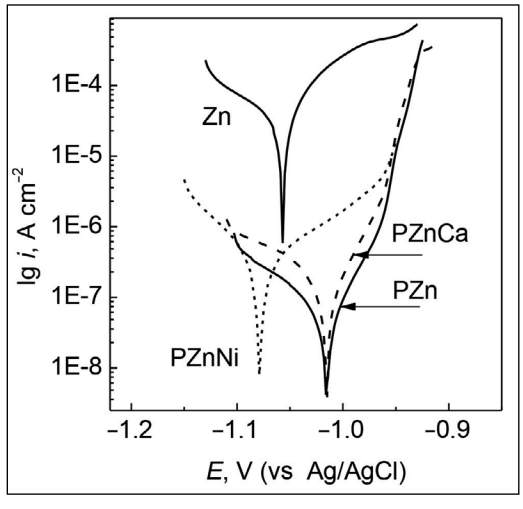

Fig. 4. Potentiodynamic polarization curves of the electrogalvanized carbon steel samples covered with PZn, PZnCa and PZnNi in a 0.5 NaCl solution at 25°C, 0.5 Mv s^{-1}

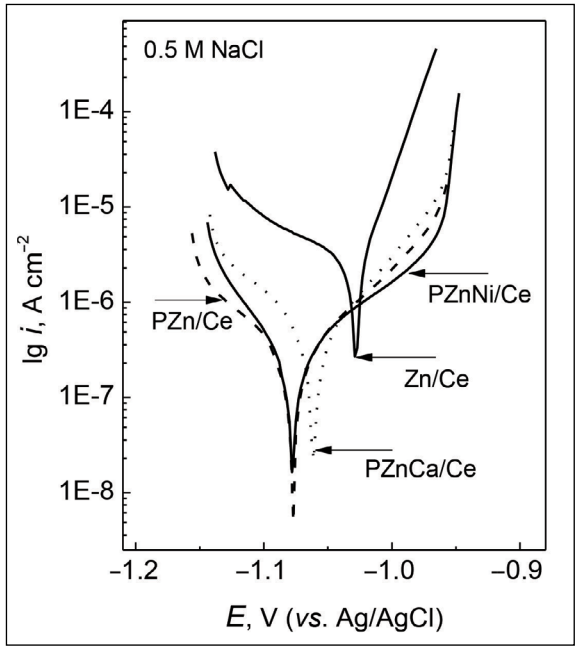

Fig. 5. Potentiodynamic polarization curves of the phosphated samples additionally coated with the conversion layers of cerium oxide in a 0.5 NaCl solution at 25°C, 0.5 Mv s^{-1}

values of R_p. The presence of Ni^{2+} in the phosphating bath improves the corrosion resistance at the base of pores. All samples additionally coated with cerium oxide layers exhibited to twofold higher R_p values, as compared with those without cerium, respectively. The protection efficiency *P*% of the samples was calculated using the following equation [5]:

$$P\% = (R_p - R_{p,m})/R_p \times 100, \quad (1)$$

where $R_{p,m}$ is the polarization resistance of the Zn electrode, R_p is the polarization resistance of phosphated Zn without/with the cerium layer. It can be stated that the phosphated samples with cerium oxide layers exhibited better protective abilities (Table 2).

The phosphate coatings act mainly as a physical barrier. The major problem in using protective coatings in aggressive environments is the possible presence of open porosity and pinholes [12, 13]. These local defects form direct paths between the corrosive environment and substrate. Corrosion of phosphate-coated electrogalvanized steel is usually localized at the pores. On the assumption that the phosphate coatings are electrochemically inert at low anodic overpotentials, the porosity *F* (%) of the coatings was calculated using the following equation [11, 12]:

$$F = (R_{p,m}/R_p) \times 10^{-|\Delta E_{corr}|/b_a}. \quad (2)$$

Here $R_{p,m}$ is the polarization resistance of the bare Zn, R_p is the polarization resistance of the phosphated Zn electrodeposits, ΔE_{corr} is the difference of the open circuit potentials E_{corr} between the Zn electrode with and without phosphate layers, and b_a is the anodic Tafel slope of the bare Zn. The open circuit potentials were measured after 0.5 h of sample immersion in a 0.5 M NaCl solution. The bare Zn electrode possessed the following characteristics: b_a = 28 mV and $R_{p,m}$ = 0.58 kΩ cm^2. It has been established that the porosity *F* of the PZn and PZnCa samples were of the order 0.2–0.5%, while that of PZnNi reached 1–2%.

EIS measurements

A more detailed study of the coatings corrosion activity during the immersion into the corrosive

Table 2. **The electrochemical parameters (corrosion current density i_{corr}, polarization resistance R_p), protection efficiency *P*% and porosity *F* of the investigated samples after 0.5 h immersion in a 0.5 M NaCl solution**

Sample	i_{corr}, A cm^{-2}	R_p, kΩ cm^2	*P*, % by Eq. 1	*F*, % by Eq. (2)
Substrate (Zn)	$4.5 \cdot 10^{-6}$	0.58	–	–
PZn	$2.8 \cdot 10^{-8}$	42.3	99.2	0.2–0.5
PZnCa	$5.6 \cdot 10^{-8}$	37.4	98.9	0.2–0.5
PZnNi	$3.1 \cdot 10^{-8}$	58.4	99.3	1–2
Zn/Ce	$1 \cdot 10^{-6}$	2.3	83.5	–
PZn/Ce	$2.7 \cdot 10^{-8}$	106.5	99.6	–
PZnCa/Ce	$4.1 \cdot 10^{-8}$	86.5	99.6	–
PZnNi/Ce	$1.8 \cdot 10^{-8}$	139.3	99.7	–

media has been done using EIS. The EIS technique is a useful tool which can provide important information on the physicochemical processes occurring on the coated sample during immersion in the corrosive media. The evolution of different parameters, such as barrier properties or polarization resistance, provides essential information on active corrosion protection properties and long-term performance. The EIS diagrams of the investigated samples after 0.5 h exposure to a 0.5 M NaCl solution are presented in Fig. 6. Two different electrical circuit models (Fig. 7a, b), which have been widely used for the analysis of impedance spectra, were selected [19, 20]. The circuit shown in Fig. 7a was used to fit the experimental data of PZn, PZnCa and PZnNi samples without the cerium oxide layer. This circuit is composed of the electrolyte resistance (R_s) and two time constants in cascade. The high frequency region of the spectrum between 10^2–10^4 Hz provides information on the phosphate coating pore resistance (R_{ph}) and capacitance (C_{ph}). The low frequency region provides information on the corrosion process characterized by charge transfer resistance (R_{ct}) and double layer capacitance (C_{dl}). In the case of PZn/Ce, PZnCa/Ce and PZnNi/Ce samples the third time constant corresponding to the contribution from the intermediate Zn and cerium oxides layers mainly appears at frequencies lower than 10^2 Hz. The information on the cerium oxides layer resistance (R_{Ce}) and capacitance (C_{Ce}) can be extracted from the fitting of EIS spectra using the equivalent circuit presented in Fig. 7b. It will be observed that at low frequency the resistive part corresponding to R_{Ce} and R_{ct} is not fully visible on EIS spectra and both time constants are overlapping.

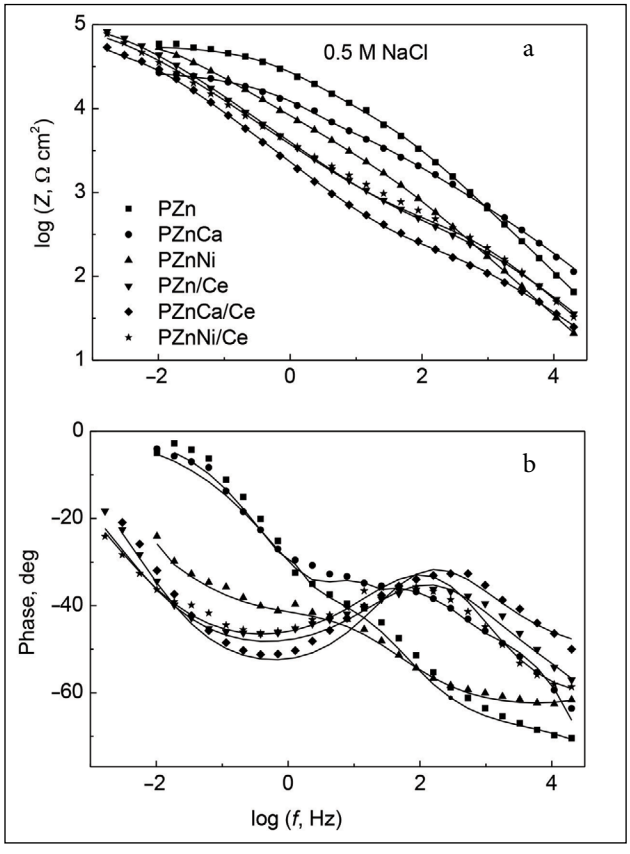

Fig. 6. Bode plots of the EIS spectra after immersion of the investigated samples in a 0.5 M NaCl solution

For fitting the data, all the capacitances in the equivalent circuits had to be replaced by a constant phase element (CPE) [21] to adapt for non-ideal behaviour. CPE instead of capacitors was actually used in the equivalent circuit models to account for a dispersive character of the time constants and inhomogeneous properties of the layers. CPE is marked as Q in the circuit description code (CDC) and it is defined by the admittance Y and the power index number n: $Y = Y_o(jw)^n$. The term n shows how far the interface is from an ideal capacitor.

Applying equivalent circuits to fit the impedance spectra, a set of fitting parameters was obtained (Table 3). It is clearly seen that after 0.5 h of

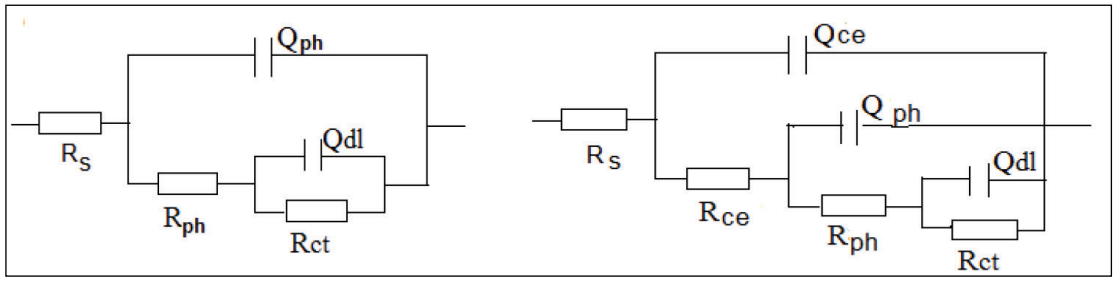

Fig. 7. Equivalent circuit models used for EIS data fitting

Table 3. **EIS parameters obtained for the investigated samples using the equivalent circuits shown in Fig. 7**

Sample	R_{Ce}, kΩ cm²	$Y_0(Q_{Ce})$ /10⁻⁵, Ω⁻¹ cm⁻² sⁿ	n (Q_{ce})	R_{ph}, kΩ cm²	$Y_0(Q_{ph})$ /10⁻⁵, Ω⁻¹ cm⁻² sⁿ	n (Q_{ph})	R_{ct}, kΩ cm²	$Y_0(Q_{ct})$ /10⁻⁵, Ω⁻¹ cm⁻² sⁿ	n (Q_{dl})
Zn	–	–	–	–	–	–	0.46	7.1	0.8
PZn	–	–	–	10.6	0.2	0.76	45.3	0.9	0.61
PZnCa	–	–	–	15.3	1.9	0.5	13.5	0.6	0.99
PZnNi	–	–	–	14.6	2.2	0.64	34.9	4.2	0.99
Zn/Ce	2.2	93	0.7	–	–	–	1.9	0.4	0.99
PZn/Ce	0.52	1.8	0.61	39.8	7.0	0.58	82.7	0.1	0.99
PZnCa/Ce	0.29	4.3	0.57	24.5	9.5	0.66	39.2	0.1	0.99
PZnNi/Ce	0.46	0.8	0.7	42.5	9.1	0.56	79.5	0.1	0.99

immersion in the 0.5 M NaCl solution the samples with cerium oxide layers PZn/Ce, PZnCa/Ce and PZnNi/Ce confer higher impedance values as compared to PZn, PZnCa and PZnNi. The results obtained demonstrate that the biggest values of R_{ct} of PZn/Ce and PZnNi/Ce were equal to 82.7 kΩ cm² and 79.5 kΩ cm², respectively. The smallest value of R_{ct} was stated for PZnCa/Ce – 39.2 kΩ cm² (Table 3).

In order to study the corrosion behaviour of the investigated samples impedance spectra were recorded for various immersion times in the 0.1 M NaCl solution. The graphics presented in Fig. 8 show the average values of R_{ph}, R_{Ce} and R_{ct} which were obtained by fitting the impedance spectra of the samples of PZnCa, PZnNi without/with cerium oxide layers.

Evolution of the phosphate coatings resistance R_{ph} during immersion of the PZnCa, PZnCa/Ce and PZnNi, PZnNi/Ce samples in the 0.1 M NaCl solution for 24 h is presented in Fig. 8a. Those samples were chosen because the R_p values of PZnCa were the lowest ones, whereas that of PZnNi was the biggest one (Table 2). At the beginning of the measurements the R_{ph} values for PZnNi and PZnNi/Ce were equal from ~70 to 100 kΩ cm², respectively. Whereas R_{ph} of the PZnCa and PZnCa/Ce samples was ~15–18 kΩ cm². A fast drop in R_{ph} values of the PZnCa, PZnCa/Ce and PZnNi samples occurs during the first 5 h followed by a monotonous decrease during the whole immersion time. Whereas PZnNi/Ce shows the highest values of R_{ph} during the whole immersion in

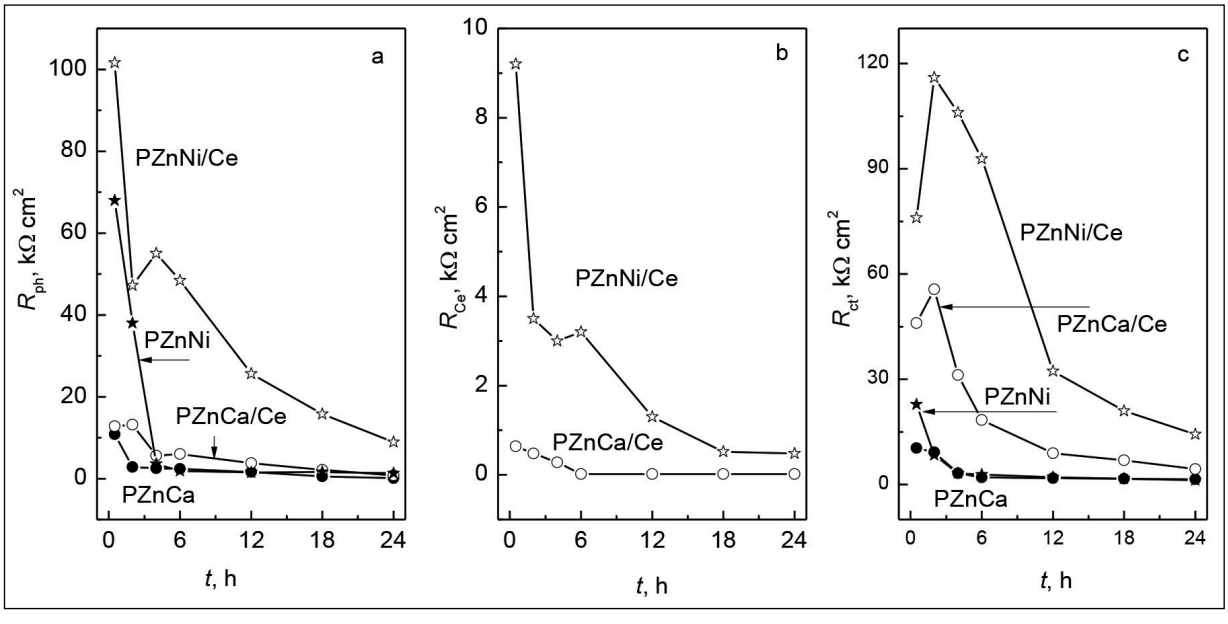

Fig. 8. Evolution of (a) the phosphate coatings pore resistance (R_{ph}), (b) the cerium oxide layer resistance (R_{Ce}) and (c) the charge transfer resistance (R_{ct}) during immersion in a 0.1 M NaCl solution

the 0.1 M NaCl solution time (Fig. 8a). The evolution of the cerium oxide layer resistance R_{Ce} for PZnCa/Ce and PZnNi/Ce samples is presented in Fig. 8b. The best performance was demonstrated for the PZnNi/Ce sample that shows the highest initial cerium oxide layer resistance ~9 kΩ cm^2. During 24 h of immersion R_{Ce} monotonously decreases to ~0.5 kΩ cm^2 for PZnNi/Ce and to ~0.05 kΩ cm^2 for PZnCa/Ce samples. A low frequency part of the impedance spectra can be used to estimate the extent of corrosion activity. The evolution of charge transfer resistance R_{ct} values is presented in Fig. 8c. The phosphate coatings are the insulating films and act mainly as a physical barrier, but the problem in the application of phosphate coatings in aggressive media is the existence of open pores. The free surface at the bottom of the pores was found to be modified in pre-treatment and post-treatment operations and in some cases was found to be more active than the clean bare metal surface [19]. With increasing immersion time, R_{ct} of the investigated samples shows the tendency to decrease. After 24 h of immersion PZnCa and PZnNi reached the lowest values of R_{ct} = 1.2–1.5 kΩ cm^2, and PZnCa/Ce reached ~4.4 kΩ cm^2. Whereas the R_{ct} value of PZnNi/Ce sample exhibited 14.3 kΩ cm^2 and was the biggest one. After 10 days of immersion R_{ct} of the most resistance PZnNi/Ce sample was equal to 6.8 kΩ cm^2, whereas R_{ct} of PZnCa/Ce was 2.4 kΩ cm^2. The experimental results suggest that the cerium oxide conversion coating imparts active corrosion protective properties to the investigated samples, reducing the corrosion progress during immersion in the saline solution.

The cerium conversion coatings can be described as a mixture of Ce(III) and Ce(IV) compounds. The presence of Ce(IV) could be due to the dismutation solid state reaction [22]:

$$Ce(OH)_3 \rightarrow CeO_2 + H_2O + ½\ H_2. \quad (3)$$

When the solution contacts the coating, tetravalent Ce compounds dissolve and Ce^{4+} ions migrate through the solution, and are reduced and precipitated as low-solubility Ce^{3+} compounds at the exposed metal surface sites. Since Ce is much less soluble in a reduced form, it then precipitates on the bare surfaces and slows corrosion [15]. The amount of Ce in the investigated samples varied from 0.8 to 2.65 at.% (Table 1). In our study on the use of cerium oxide films on the amorphous phosphate coating on carbon steel it was stated that the percentage of Ce^{4+} to total Ce was equal to ~50 % [23]. SEM images of the cross-section (Fig. 3) revealed the structural defects like open and closed pores in the PZnNi coating. It was stated that the more porous (F = ~1–2%) PZnNi/Ce coating exhibited better protective abilities in a chloride-contaminated solution. Therefore, Ce^{4+} ions are able to penetrate into the substrate, which is the electrogalvanized steel, through the open pores of the PZnNi layer. To summarize the results of electrochemical and SEM measurements, the more porous PZnNi/Ce coating on galvanized steel demonstrated effective protective properties in the chloride-contaminated solution.

CONCLUSIONS

The investigated coatings systems on the electrogalvanized steel consisted of PZn, PZnCa and PZnNi additionally coated with cerium oxide layers. The SEM studies of the microstructure have revealed that the cerium oxide conversion coating on all phosphated samples exhibits a cracked 'dried river' morphology. The cross-section images of the PZnNi phosphate coating confirmed the presence of the structural defects like open and closed pores in this layer.

The results of potentiodynamic polarization measurements have revealed that all investigated phosphate coatings, which act mainly as a physical barrier, improved the protection efficiency of electrogalvanized steel samples in a 0.5 M NaCl solution. The experimental results suggest that the cerium oxides conversion coating imparts active corrosion protective properties to the investigated samples, reducing the corrosion progress during immersion in the saline solution. The all phosphated samples with cerium layers exhibited better protective abilities.

SEM images of the cross-section revealed the structural defects like open and closed pores in the PZnNi coating. It was stated that the more porous (F = ~1–2%) PZnNi/Ce coating exhibited the best protective abilities in a chloride-contaminated solution. Therefore, Ce^{4+} ions are able to penetrate into the substrate, which is the electrogalvanized steel, through the open pores of the PZnNi

layer. To summarize the results of electrochemical and SEM measurements, the more porous PZnNi/Ce coating on galvanized steel demonstrated effective protective properties in the chloride-contaminated solution.

Received 3 March 2020
Accepted 17 March 2020

References

1. J. E. Svensson, L. G. Johansson, *Corros. Sci*., **34**, 721 (1993).
2. J. Zhao, G. S. Frankel, R. L. McCreery, *J. Electrochem. Soc*., **145**, 2258 (1998).
3. W. Machu, *Die Phosphatierung*, Verlag Chemie (1950).
4. D. B. Freeman, *Phosphating and Metal Pre-Treatment*, Woodhead-Faulkner Ltd., Cambrige, England (1986).
5. D. Weng, P. Jokiel, A. Uebleis, H. Boehni, *Surf. Coat. Technol*., **88**, 147 (1996).
6. K. Ogle, A. Tomandl, N. Meddahi, M. Wolpers, *Corros. Sci*., **46**, 979 (2004).
7. A. Tomandl, M. Wolpers, K. Ogle, *Corros. Sci*., **46**, 997 (2004).
8. F. Simescu, H. Idrissi, *Corros. Sci*., **51**, 833 (2009).
9. V. F. C. Lins, G. F. A. Reis, C. R. Araujo, T. Matencio, *Surf. Sci*., **253**, 2875 (2006).
10. D. Zimmermann, A. G. Munoz, J. W. Schultze, *Electrochim. Acta*, **48**, 3267 (2003).
11. J. Donofrio, *Met. Finish*., **98**, 57 (2000).
12. J. Creus, H. Mazille, H. Idrissi, *Surf. Coat. Technol*., **130**, 224 (2000).
13. C. Liu, Q. Bi, A. Leyland, A. Matthews, *Corros. Sci*., **45**, 1257 (2003).
14. B. R. Hinton, L. Wilson, *Corros. Sci*., **29**, 967 (1989).
15. R. G. Buchheit, S. B. Mamidipally, P. Schmutz, H. Guan, *Corros. Sci*., **58**, 3 (2002).
16. Y. Kobayashi, N. Yamashita, Y. Fujiwara, M. Yamashita, *J. Surf. Fin. Soc. Jpn*., **55**, 276 (2004).
17. Y. Kobayashi, Y. Fujiwara, *Electrochim. Acta*, **51**, 4236 (2006).
18. B. A. Boukamp, *J. Electrochem. Soc*., **142**, 1885 (1995).
19. V. de Freitas Cunha Lins, G. F. de Andrade Reis, C. R. de Araujo, T. Matencio, *Appl. Surf. Sci*., **253**, 2875 (2006).
20. K. Y. Yasakau, J. Carneiro, M. L. Zheludkevich, M. G. S. Ferreira, *Surf. Coat. Technol*. **246**, 6 (2014).
21. K. Jütnerr, *Electrochim. Acta*, **35**, 1501 (1990).
22. M. A. Arenas, J. J. de Damborenea, *Surf. Coat. Technol*. **187**, 320 (2004).
23. O. Girčienė, L. Gudavičiūtė, A. Selskis, V. Jasulaitienė, S. Šakirzanovas, R. Ramanauskas, *Chemija*, **26**(**3**), 175 (2015).

O. Girčienė, L. Gudavičiūtė, A. Selskienė, A. Kirdeikienė, R. Ramanauskas

FOSFATUOTO CINKUOTO PLIENO, PAPILDOMAI PADENGTO CERIO OKSIDŲ KONVERSINE DANGA, ANTIKOROZINĖS ELGSENOS TYRIMAI

S a n t r a u k a

Tirta fosfatuotų cinkuoto anglinio plieno pavyzdžių (PZn, PZnCa ir PZnNi), papildomai padengtų konversinio cerio oksidų dangomis, korozinė elgsena 0,1–0,5 M NaCl tirpaluose. Pasirinktų pavyzdžių sudėtis ir struktūra buvo tirti skenuojančiu elektroniniu mikroskopu SEM, korozinė elgsena nustatyta elektrocheminiais tyrimų metodais (voltamperometrija ir EIS). Gauti tyrimų duomenys parodė, kad visi pavyzdžiai, padengti papildomu cerio oksidų sluoksniu, pasižymi geresnėmis antikorozinėmis savybėmis. Apibendrinus gautus tyrimų rezultatus matyti, kad Ce^{4+} jonai per fosfatinės dangos poras pasiekia pagrindą (cinkuotas anglinis plienas), todėl tarp visų tirtų pavyzdžių labiau poringa (F = ~1–2 %) PZnNi/Ce danga pasižymi geriausiomis apsauginėmis savybėmis chloro jonais užterštame tirpale.